

Electronic supplementary information

A Theoretical Study on the Surface and Interfacial Properties of Ni₃P for Hydrogen Evolution Reaction†

Jun Hu,^{a,b} Shunli Zheng,^a Xin Zhao,^{a*} Xin Yao^a and Zhong Chen^{a*}

^a School of Materials Science and Engineering, Nanyang Technological University, 50 Nanyang Avenue, Singapore 639798

^b School of Chemical Engineering, Northwest University, Xi'an, P. R. China 710069;

Corresponding Authors

*E-mail: xinzhao@ntu.edu.sg; (X. Zhao).

*E-mail: ASZChen@ntu.edu.sg; (Z. Chen).

ORCID

J. Hu: 0000-0002-3075-9291

Z. Chen: 0000-0001-7518-1414

Table S1. The total energies of surfaces with different terminations (total 19 surfaces). The terminations positions are shown in [Figure S15](#).

Surface	Formula	Area / Å ²	Total energy/ eV
(001)A	Ni ₅₆ P ₁₆	80.174116	-78766.88929
(001)B	Ni ₅₂ P ₂₀	80.174116	-74075.66493
(001)C	Ni ₄₈ P ₁₆	80.174116	-67924.17380
(100)A	Ni ₅₆ P ₁₆	78.544488	-78766.15099
(100)B	Ni ₄₈ P ₁₆	78.544488	-67928.51171
(100)C	Ni ₅₂ P ₂₀	78.544488	-74074.47540
(100)D	Ni ₆₀ P ₂₀	78.544488	-84916.51426
(011)A	Ni ₁₂₀ P ₃₂	179.585220	-168361.32813
(011)B	Ni ₉₆ P ₃₂	179.585220	-135844.61661
(011)C	Ni ₇₂ P ₃₂	179.585220	-103322.72740
(110)A	Ni ₄₈ P ₁₆	55.275856	-67933.95777
(110)B	Ni ₄₀ P ₁₆	55.275856	-57097.49211
(110)C	Ni ₄₈ P ₁₆	55.275856	-67939.90186
(110)D	Ni ₃₆ P ₁₆	55.275856	-51675.46485
(110)E	Ni ₅₆ P ₁₆	55.275856	-78775.02379
(111)A	Ni ₆₆ P ₂₄	97.518636	-93766.44809
(111)B	Ni ₆₀ P ₂₂	97.518636	-85272.05490
(111)C	Ni ₆₆ P ₂₀	97.518636	-93038.63093
(111)D	Ni ₆₀ P ₂₀	97.518636	-84909.17993

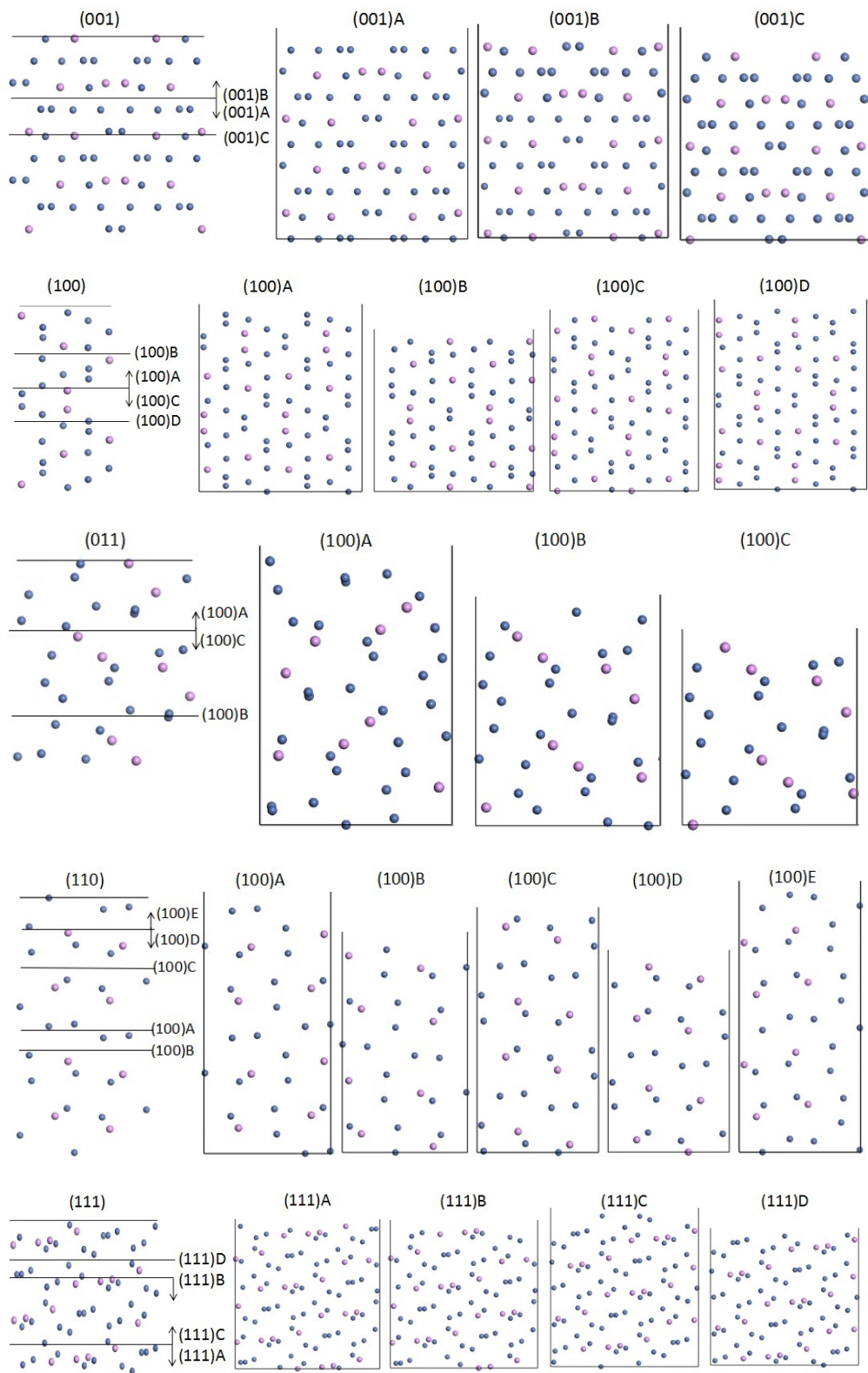


Figure S1. The terminated position of different surfaces.

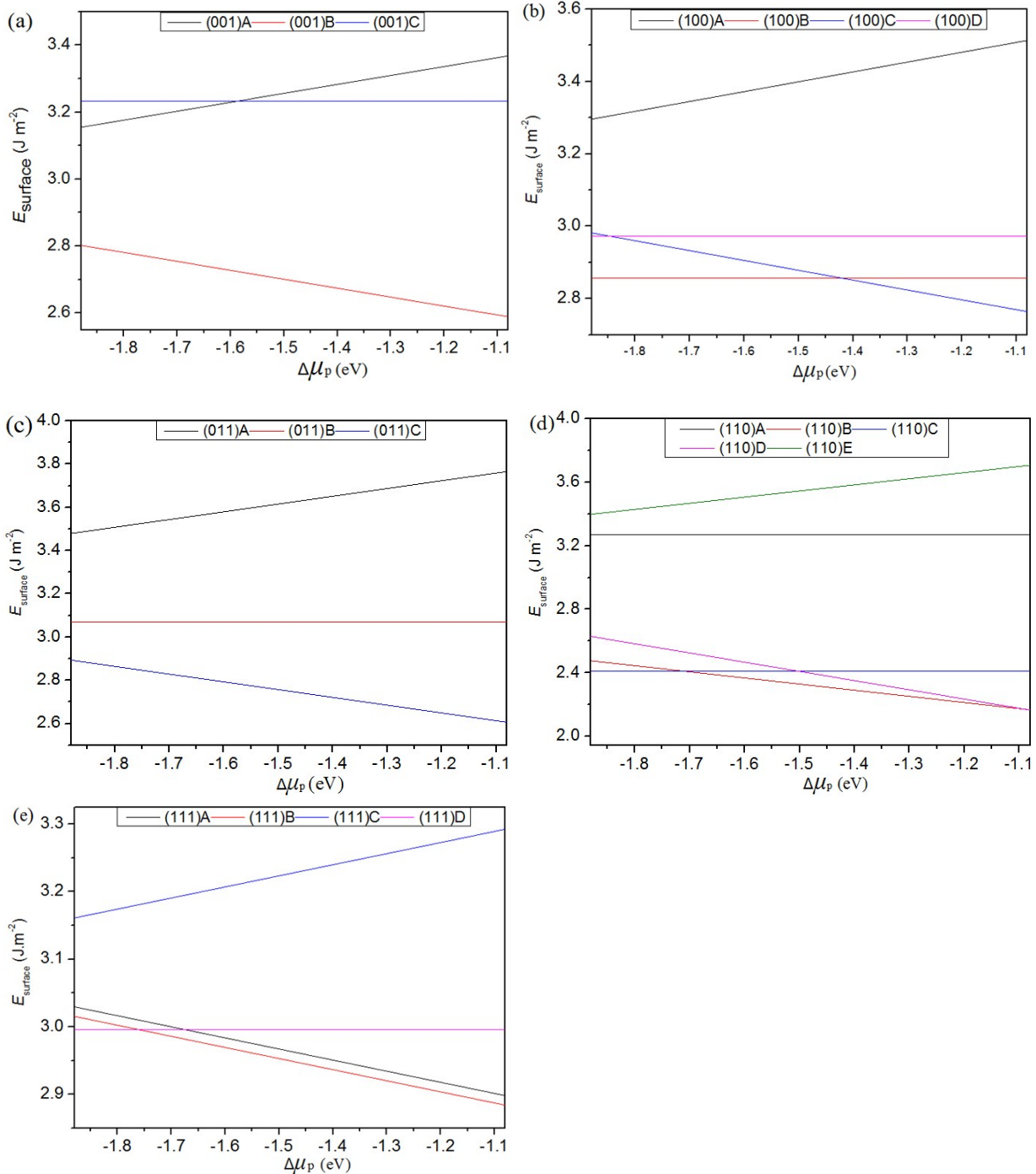


Figure S2. The energy of surfaces with different terminations. (a) the (001) facet; (b) the (100) facet; (c) the (011) facet; (d) the (110) facet; (e) the (111) facet. The lowest energy surfaces for every facets are shown in Figure 1(b).

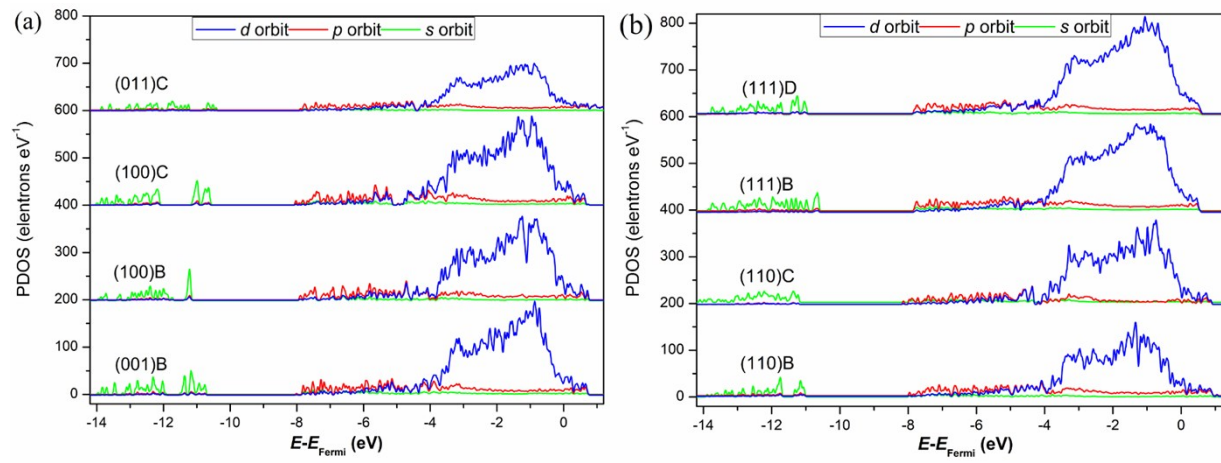


Figure S3. The calculated electronic characteristics of Ni₃P with different low-index surfaces (a) PDOS of the (001)B, (100)B, (100)C, (011)C; (b) PDOS of the (110)B, (110)C, (111)B and (111)D.

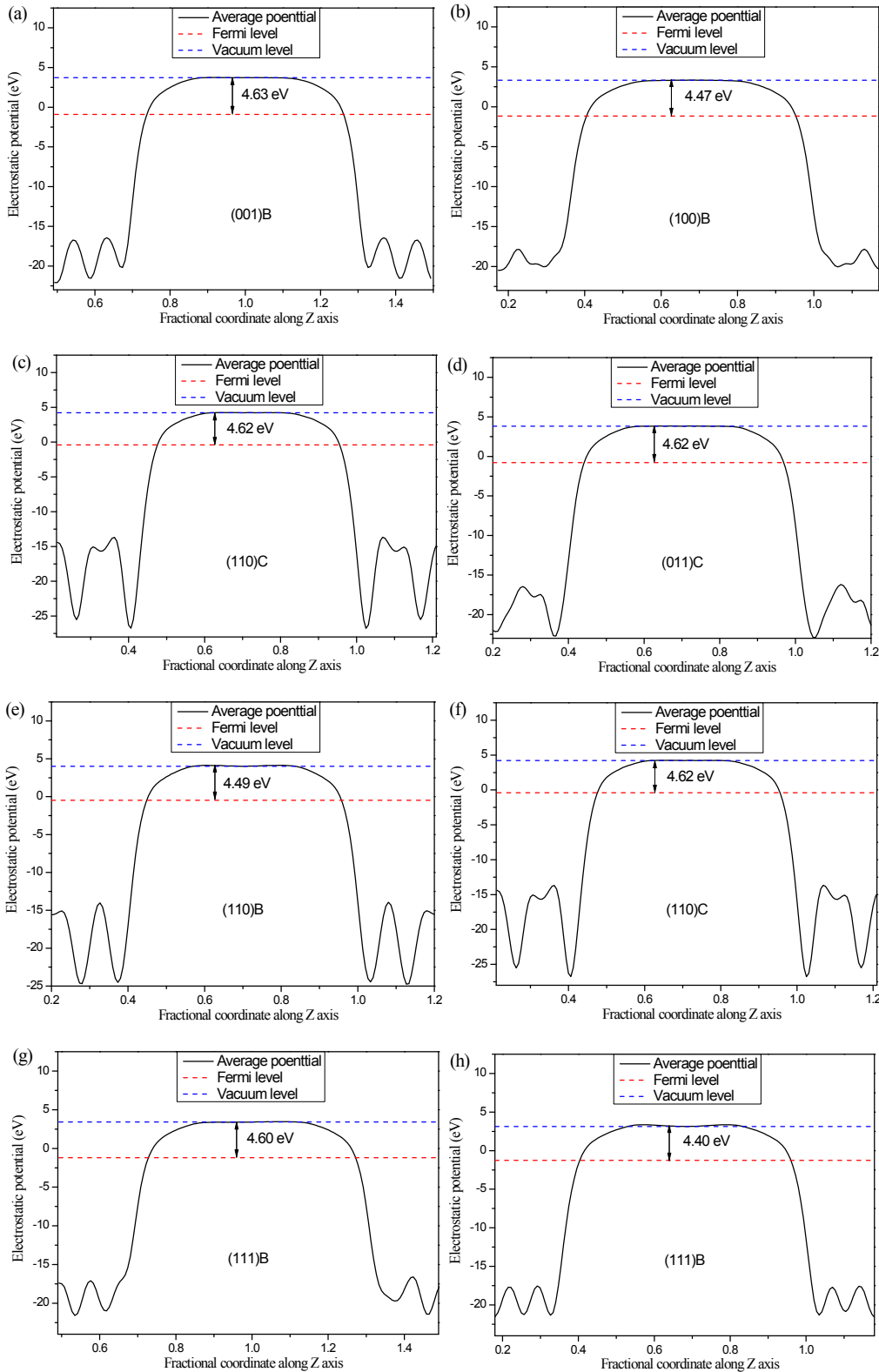


Figure S4. Work functions of Ni₃P with different low-index surfaces (a) the (001)B; (b) the (100)B; (c) the (100)C; (d) the (011)C; (e) the (110)B; (f) the (110)C; (g) the (111)B and (h) the (111)D.

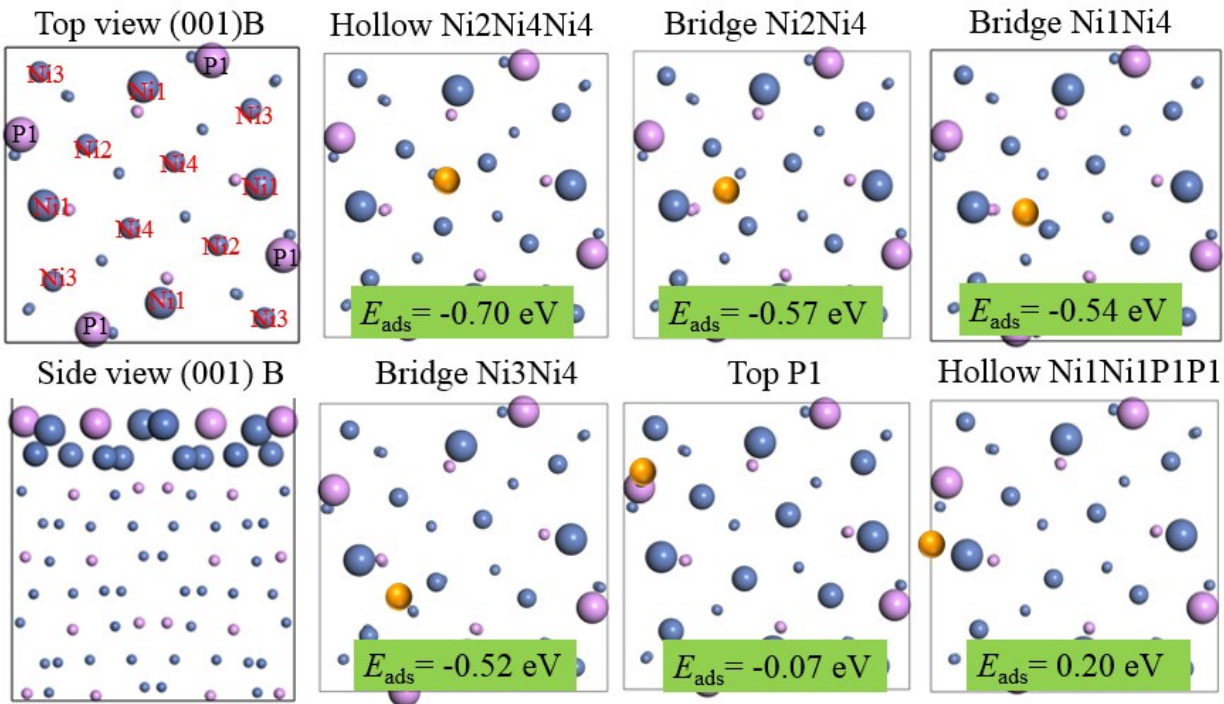


Figure S5. The stable adsorption structures and energies of H involved in a water splitting process on the (001)B surface. The atoms in the first layer of surface are shown in large spheres, second layer of surface are shown in medium-sized spheres and the others are shown in small spheres. In the cell, yellow spheres stand for H atoms, violet spheres stand for P atoms and blue spheres stand for Ni atoms.

Table S2. Stable adsorption structures of H on the (001)B surface.

H position before Optimization	H position after Optimization	Total energy/ eV	Adsorption energy/ eV
Top Ni1	Bridge Ni1Ni4	-74091.97816	-0.53923
Top P1	Top P1	-74091.50588	-0.06695
Top Ni2	Bridge Ni2Ni4	-74092.01184	-0.57291
Top Ni3	Bridge Ni3Ni4	-74091.96222	-0.52329
Hollow Ni2Ni4Ni4	Hollow Ni2Ni4Ni4	-74092.13475	-0.69582
Bridge Ni1Ni4	Bridge Ni1Ni4	-74091.97976	-0.54083
Bridge Ni2Ni4	Hollow Ni2Ni4Ni4	-74092.00891	-0.56998
Bridge Ni1P1	Hollow Ni1Ni1P1P1	-74091.23480	0.20413

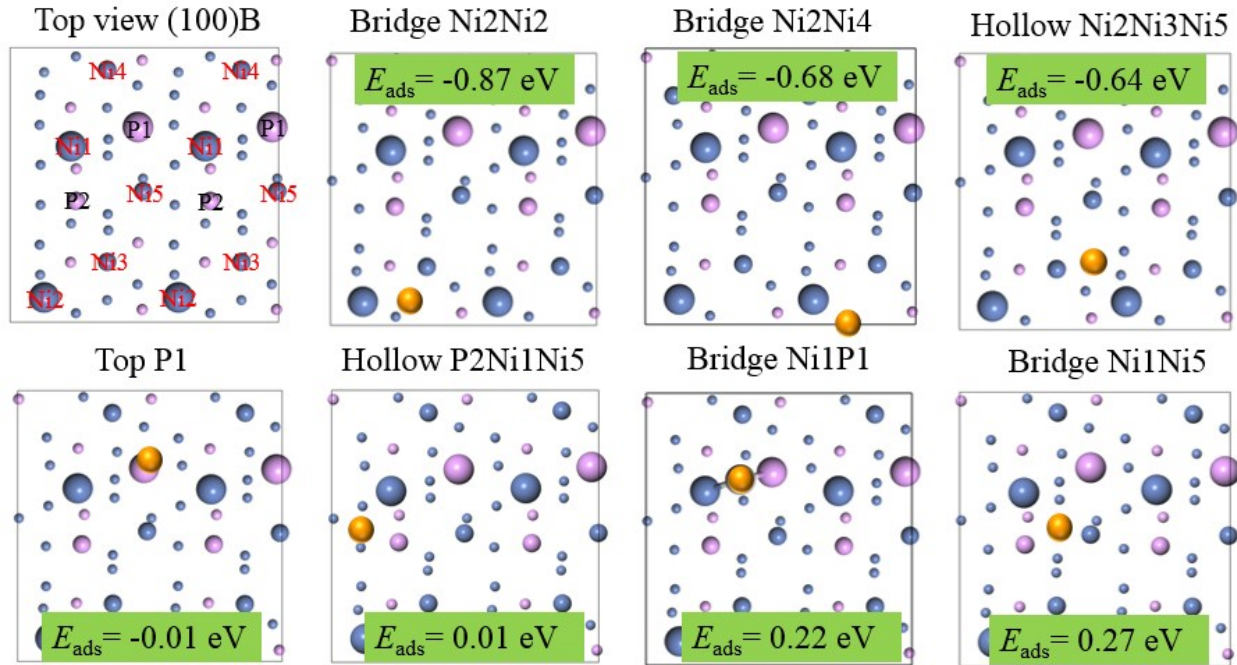


Figure S6. Stable adsorption structures and energies of H involved in a water splitting process on the (100) B surface.

Table S3. Stable adsorption structures of H on the (100)B surface.

H position before Optimization	H position after Optimization	Total energy/ eV	Adsorption energy/ eV
Top Ni2	Bridge Ni2Ni4	-59450.04985	-0.67970
Top Ni5	Hollow Ni2Ni3Ni5	-59449.96916	-0.59912
Bridge Ni1P1	Bridge Ni1P1	-59449.15264	0.21752
Top P1	Top P1	-59449.37541	-0.00525
Hollow Ni1Ni3Ni5	Hollow Ni2Ni3Ni5	-59450.00777	-0.63762
Hollow P2Ni1Ni5	Bridge Ni1Ni5	-59449.10466	0.26545
Hollow P2Ni3Ni5	Hollow Ni2Ni3Ni5	-59450.00861	-0.63846
Hollow P2Ni1Ni5	Hollow P2Ni1Ni5	-59449.36095	0.00921
Top P2	Hollow P2Ni1Ni5	-59449.36083	0.00933

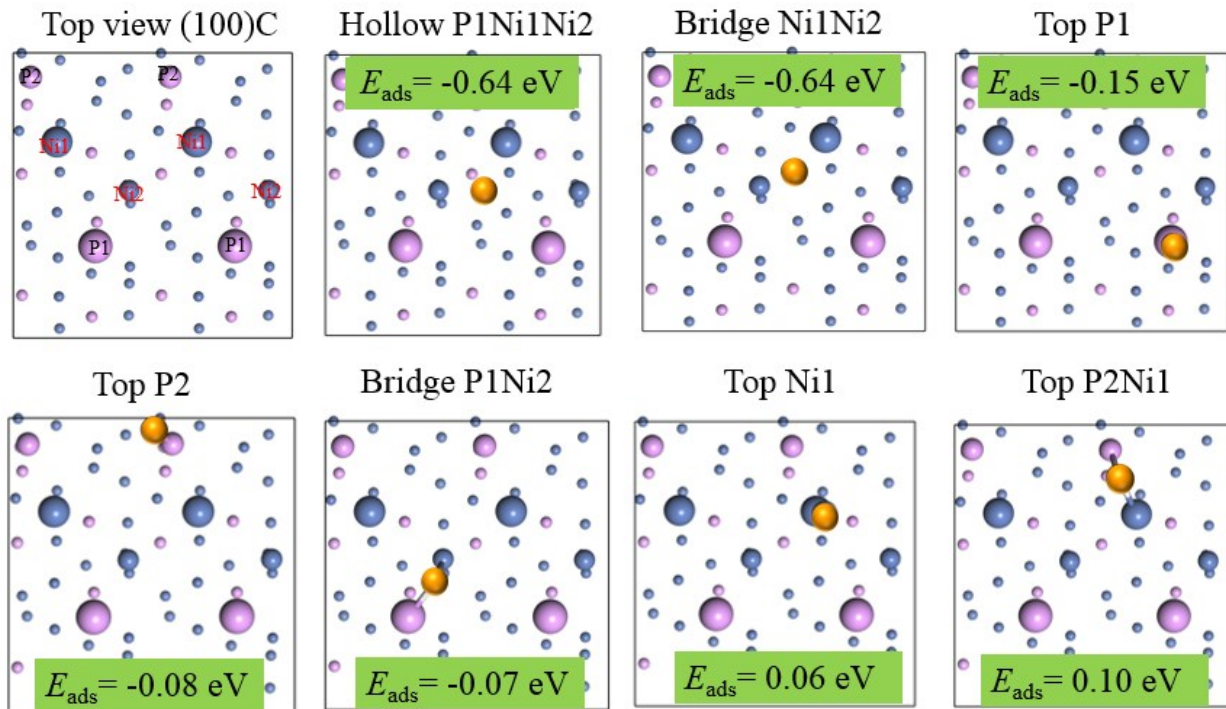


Figure S7. Stable adsorption structures and energies of H involved in a water splitting process on the (100)C surface.

Table S4 The detail information about stable adsorption structures of H on (100)C surface.

H position before Optimization	H position after Optimization	Total energy/ eV	Adsorption energy/ eV
Top P1	Top P1	-74090.39862	-0.14922
Top P2	Top P2	-74090.32506	-0.07566
Top Ni1	Top Ni1	-74090.18839	0.06101
Top Ni2	Bridge Ni1Ni2	-74090.88513	-0.63573
Bridge Ni1Ni2	Bridge Ni1Ni2	-74090.73997	-0.49057
Bridge P1Ni1	Hollow P1Ni1Ni2	-74090.89217	-0.64277
Bridge P1Ni2	Bridge P1Ni2	-74090.32386	-0.07446
Bridge P2Ni1	Bridge P2Ni1	-74090.14643	0.10297
Hollow Ni1Ni2P2	Bridge Ni1Ni2	-74090.88865	-0.63925
Hollow P1Ni1Ni2	Bridge Ni1Ni2	-74090.73956	-0.49016

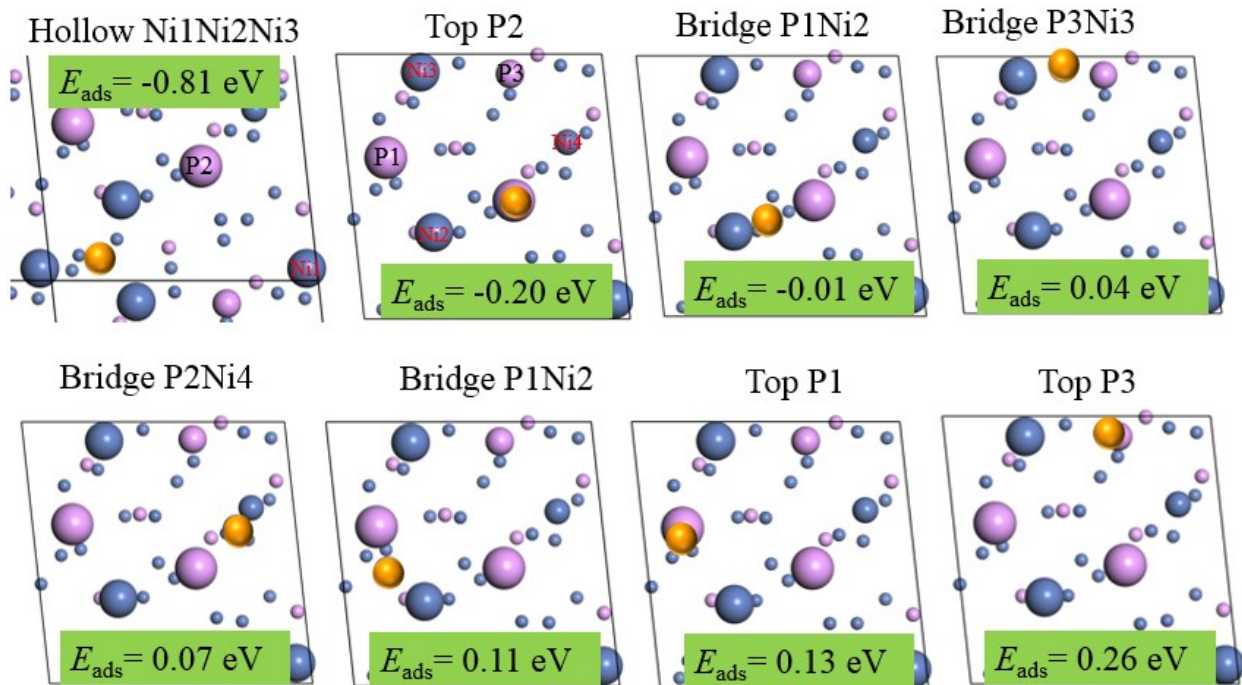


Figure S8. Stable adsorption structures and energies of H involved in a water splitting process on the (011)C surface.

Table S5. Stable adsorption structures of H on the (011)C surface.

H position before Optimization	H position after Optimization	Total energy/ eV	Adsorption energy/ eV
Top P1	Top P1	-42835.80998	0.12873
Top P2	Top P2	-42836.13657	-0.19786
Top P3	Top P3	-42835.67943	0.25928
Bridge P1Ni3	Hollow Ni1Ni2Ni3	-42836.75153	-0.81282
Bridge P2Ni2	Bridge P2Ni2	-42835.95175	-0.01304
Bridge P2Ni4	Bridge P2Ni4	-42835.87108	0.06763
Bridge P1Ni2	Bridge P1Ni2	-42835.82376	0.11495
Bridge P3Ni3	Bridge P3Ni3	-42835.89712	0.04159
Bridge P3Ni4	Hollow Ni1Ni2Ni3	-42836.74833	-0.80962
Hollow Ni1Ni2Ni3	Hollow Ni1Ni2Ni3	-42836.74467	-0.80596

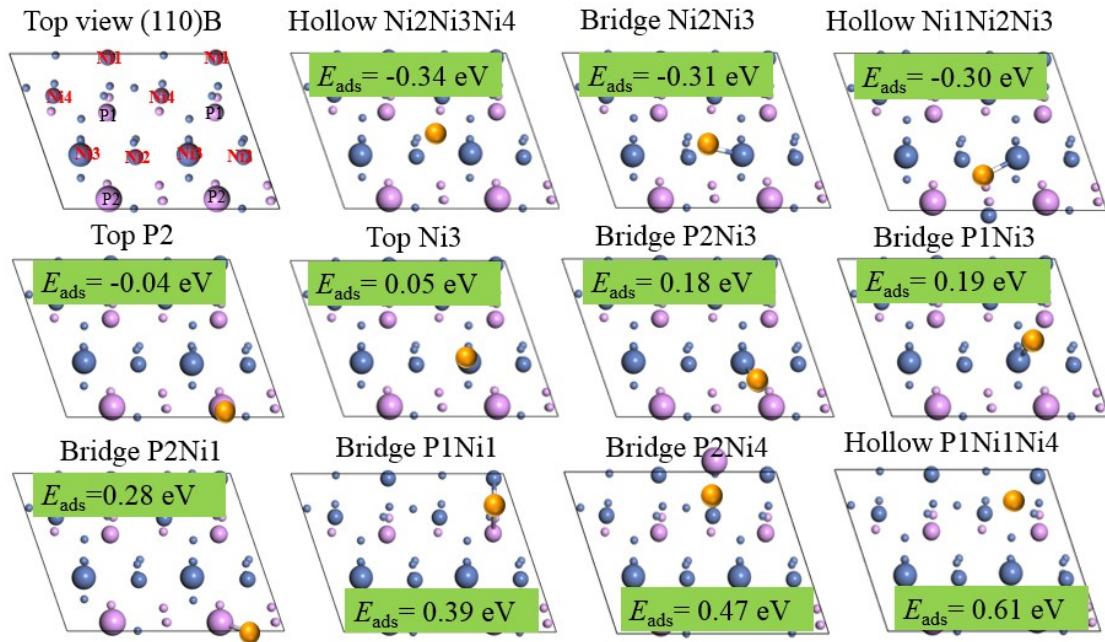


Figure S9. Stable adsorption structures and energies of H involved in a water splitting process on the (110)B surface.

Table S6. Stable adsorption structures of H on the (110)B surface.

H position before Optimization	H position after Optimization	Total energy/ eV	Adsorption energy/ eV
Top P1	Top Ni3	-57113.21824	0.04787
Top P2	Top P2	-57113.30240	-0.03629
Top Ni1	Top Ni1	-57113.02690	0.23921
Top Ni2	Bridge Ni2Ni3	-57113.57949	-0.31338
Top Ni3	Bridge Ni2Ni3	-57113.57615	-0.31004
Top Ni4	Hollow Ni2Ni3Ni4	-57113.59458	-0.32847
Bridge Ni2Ni3	Bridge Ni2Ni3	-57113.55537	-0.28926
Bridge Ni3Ni4	Hollow Ni2Ni3Ni4	-57113.60144	-0.33533
Bridge P1Ni1	Bridge P1Ni1	-57112.87719	0.38892
Bridge P1Ni2	Hollow Ni2Ni3Ni4	-57113.59027	-0.32416
Bridge P1Ni3	Bridge P1Ni3	-57113.08009	0.18602
Bridge P1Ni4	Hollow Ni2Ni3Ni4	-57113.59982	-0.33371
Bridge P2Ni1	Bridge P2Ni1	-57112.98617	0.27994
Bridge P2Ni2	Bridge Ni2Ni3	-57113.57959	-0.31348
Bridge P2Ni3	Bridge P2Ni3	-57113.08185	0.18426
Bridge P2Ni4	Bridge P2Ni4	-57112.79494	0.47117
Hollow P1Ni1Ni4	Hollow P1Ni1Ni4	-57112.65561	0.61050
Hollow P1Ni2Ni3	Hollow Ni2Ni3Ni4	-57113.59477	-0.32866
Hollow P1Ni3Ni4	Hollow Ni2Ni3Ni4	-57113.60592	-0.33981
Hollow P2Ni1Ni2	Hollow Ni1Ni2Ni3	-57113.56835	-0.30224
Hollow P2Ni1Ni3	Hollow Ni1Ni2Ni3	-57113.56592	-0.29981
Hollow P2Ni1Ni4	Bridge P2Ni1	-57112.98730	0.27881
Hollow P2Ni2Ni3	Top Ni3	-57113.14743	0.11868

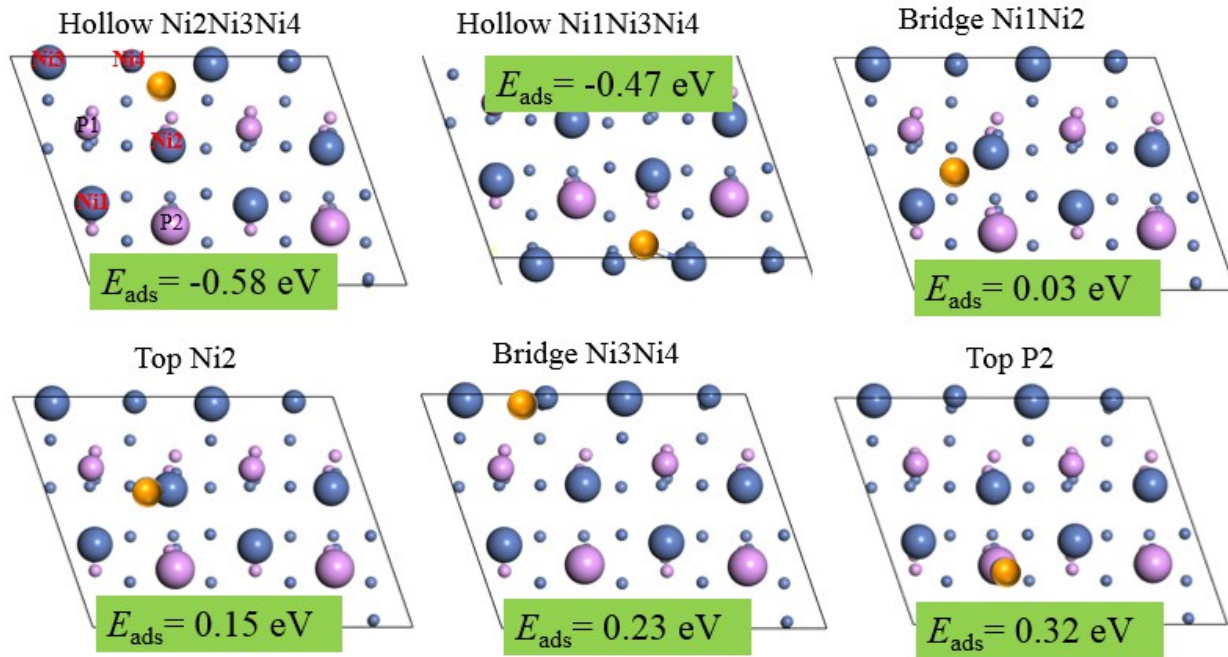


Figure S10. Stable adsorption structures and energies of H involved in a water splitting process on the (110)C surface.

Table S7. Stable adsorption structures of H on the (110)C surface.

H position before Optimization	H position after Optimization	Total energy/ eV	Adsorption energy/ eV
Top P1	Hollow Ni1Ni3Ni4	-67956.14729	-0.47142
Top P2	Top P2	-67955.35141	0.32446
Top Ni1	Hollow Ni2Ni3Ni4	-67956.16228	-0.48641
Top Ni2	Hollow Ni2Ni3Ni4	-67956.26029	-0.58442
Top Ni3	Hollow Ni2Ni3Ni4	-67956.25341	-0.57754
Top Ni4	Hollow Ni2Ni3Ni4	-67956.25308	-0.57721
Bridge P1Ni3	Hollow Ni1Ni3Ni4	-67956.14605	-0.47019
Bridge P1Ni4	Bridge Ni3Ni4	-67955.45007	0.22579
Bridge P2Ni1	Bridge Ni1Ni2	-67955.64116	0.03470
Bridge P2Ni2	Top Ni2	-67955.52104	0.15482
Bridge P2Ni4	Hollow Ni2Ni3Ni4	-67956.24708	-0.57121
Hollow NI2Ni3Ni4	Hollow Ni2Ni3Ni4	-67956.23930	-0.56344
Hollow P1Ni1Ni2	Bridge Ni1Ni2	-67955.62408	0.05179
Hollow P1Ni1ni3	Hollow Ni1Ni3Ni4	-67956.14192	-0.46606
Hollow P2Ni1Ni2	Bridge Ni1Ni2	-67955.62826	0.04760
Hollow P2Ni2Ni4	Hollow Ni2Ni3Ni4	-67956.23191	-0.55605
Hollow P2Ni3Ni4	Bridge Ni3Ni4	-67955.43712	0.23875

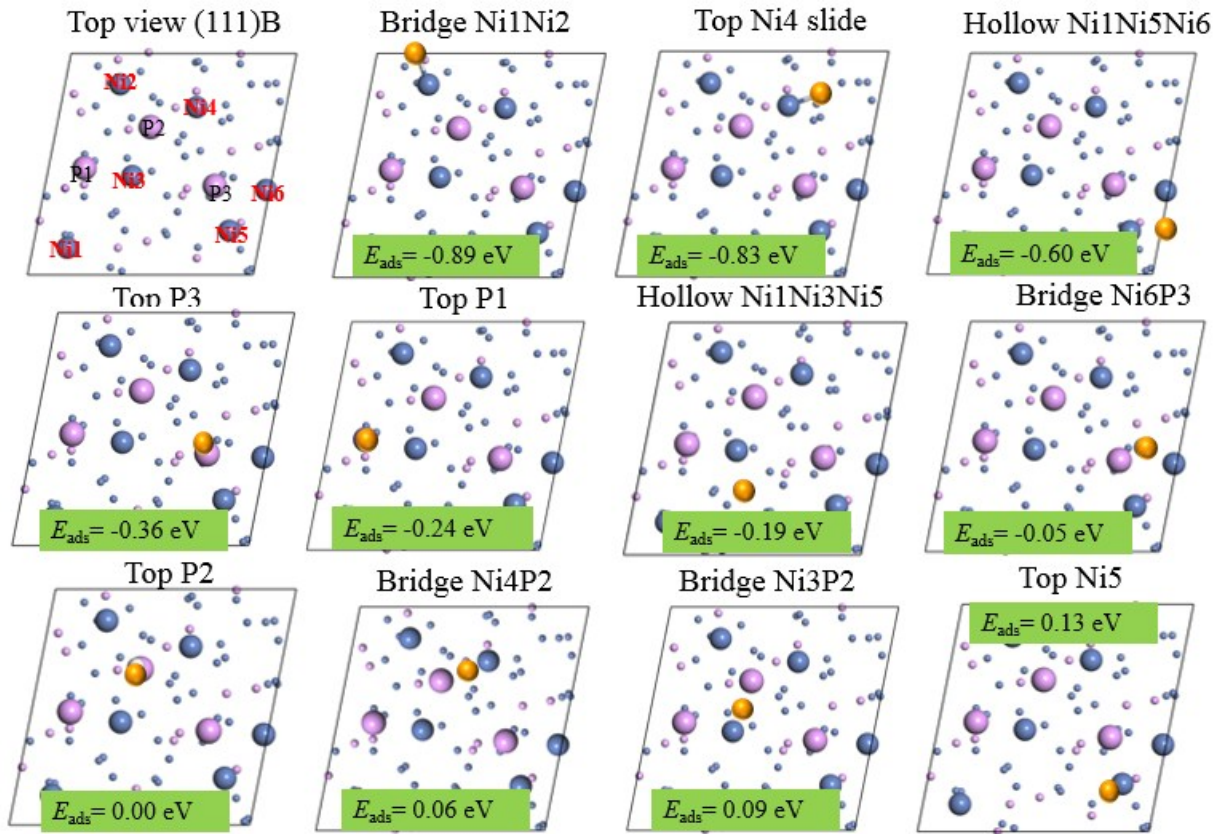


Figure S11. Stable adsorption structures and energies of H involved in a water splitting process on the (111)B surface.

Table S8. Stable adsorption structures of H on the (111)B surface.

H position before Optimization	H position after Optimization	Total energy/ eV	Adsorption energy/ eV
Top P1	Top P1	-85288.07324	-0.24434
Top P2	Top P2	-85287.82638	0.00252
Top P3	Top P3	-85288.18649	-0.35759
Top P4	Top Ni5	-85287.69635	0.13255
Top Ni1	Bridge Ni1Ni2	-85288.71252	-0.88362
Top Ni2	Bridge Ni1Ni2	-85288.71441	-0.88551
Top Ni3	Hollow Ni1Ni3Ni5	-85288.02377	-0.19486
Top Ni4	Top Ni4	-85288.65711	-0.82821
Top Ni5	Hollow Ni1NI5ni6	-85288.42849	-0.59959
Top Ni6	Hollow Ni1NI5ni6	-85288.42971	-0.60081
Bridge Ni3P2	Bridge Ni3P2	-85287.73497	0.09393
Bridge Ni4P2	Bridge Ni4P2	-85287.77178	0.05713
Bridge Ni5P3	Top Ni5	-85287.67238	0.15652
Bridge Ni6P3	BridgeNi6P3	-85287.87888	-0.04998
Bridge P1P2	Bridge Ni3P2	-85287.73423	0.09467
Hollow P3Ni5Ni6	Hollow Ni1NI5ni6	-85288.43380	-0.60490
Hollow P2Ni2Ni4	Bridge Ni1Ni2	-85288.71306	-0.88416

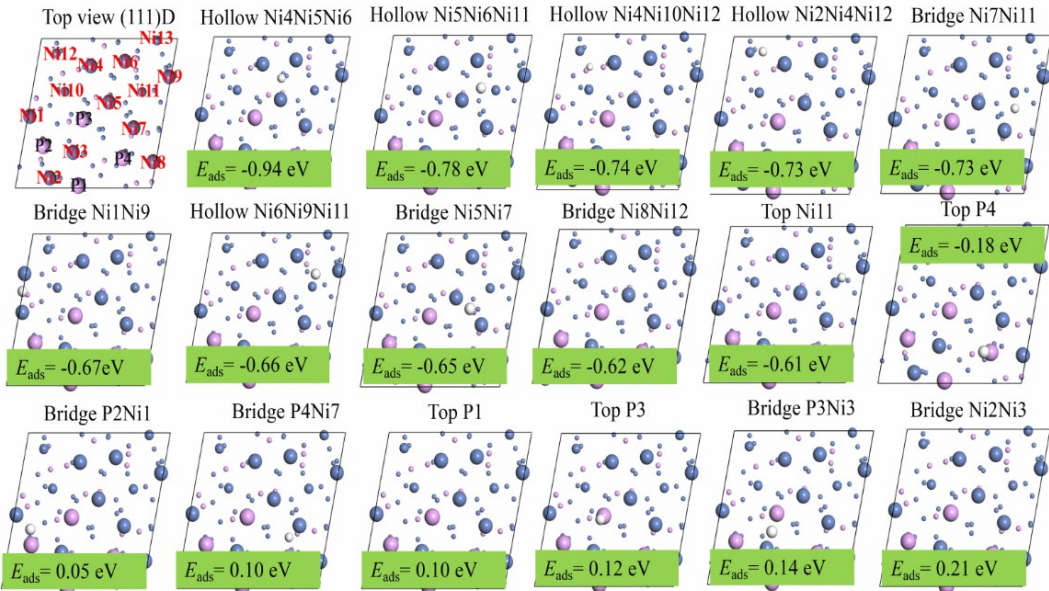


Figure S12. Stable adsorption structures and energies of H involved in a water splitting process on the (111)D surface.

Table S9. Stable adsorption structures of H on the (111)D surface.

H position before	H position after	Total energy/ eV	Adsorption
Top P1	Top P1	-84924.85394	0.09999
Top P2	Bridge P2Ni1	-84924.89968	0.05424
Top P3	Top P3	-84924.83060	0.12333
Top P4	Top P4	-84925.13768	-0.18375
Top Ni1	Bridge Ni1Ni9	-84925.61315	-0.65922
Top Ni2	Hollow Ni2Ni8Ni12	-84925.53355	-0.57962
Top Ni3	Top Ni3	-84924.70437	0.24956
Top Ni4	Hollow Ni4Ni5Ni6	-84925.89482	-0.94089
Top Ni5	Hollow Ni5Ni6Ni11	-84925.73176	-0.77784
Top Ni6	Hollow Ni4Ni5Ni6	-84925.89480	-0.94087
Top Ni7	Bridge Ni7Ni11	-84925.67173	-0.71780
Top Ni8	Bridge Ni2Ni8Ni12	-84925.57582	-0.62190
Top Ni9	Bridge Ni1Ni9	-84925.61998	-0.66605
Top Ni10	Hollow Ni4Ni10Ni12	-84925.69720	-0.74327
Top Ni11	Top Ni11	-84925.56402	-0.61009
Bridge P2Ni5	Hollow Ni5Ni6Ni11	-84925.73742	-0.78349
Bridge Ni4Ni5	Hollow Ni4Ni5Ni6	-84925.89469	-0.94076
Bridge Ni4Ni6	Hollow Ni4Ni5Ni6	-84925.89306	-0.93914
Bridge Ni5Ni6	Hollow Ni4Ni5Ni6	-84925.88887	-0.93495
Bridge Ni5Ni7	Bridge Ni5Ni7	-84925.60267	-0.64875
Bridge Ni6Ni9	Hollow Ni6Ni9Ni11	-84925.61044	-0.65651
Bridge Ni7Ni8	Bridge Ni7Ni11	-84925.68102	-0.72710
Bridge P1Ni2	Hollow Ni2Ni4Ni12	-84925.68202	-0.72807
Bridge P1Ni3	Bridge Ni2Ni3	-84924.74055	0.21337
Bridge P2Ni3	Bridge Ni3P3	-84924.81477	0.13915
Bridge P3Ni2	Hollow Ni2Ni4Ni12	-84925.68857	-0.73464
Bridge P3Ni3	Bridge Ni2Ni3	-84924.73566	0.21827
Bridge P4Ni7	Bridge P4Ni7	-84924.85509	0.09884

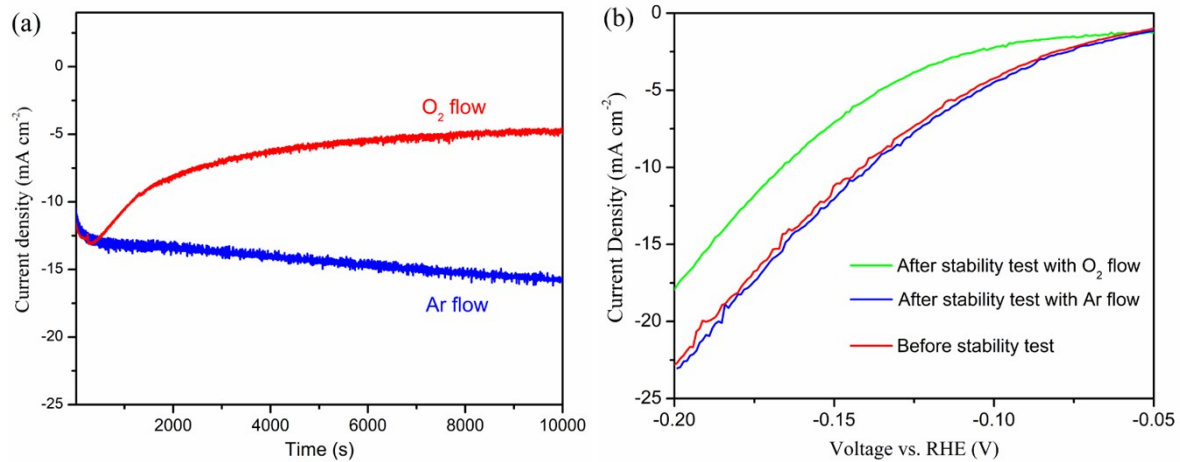


Figure S13. (a) the current of Ni_3P when applied -0.13 V potential at room temperature in 0.5 M H_2SO_4 solutions; (b) the linear sweep voltammetry with a scan rate of 5 mV s^{-1} at room temperature in 0.5 M H_2SO_4 solutions. Herein, the Ni_3P film were prepared by metal-organic decomposition method based on Ref. S1. $\text{NiCl}_2 \cdot 6\text{H}_2\text{O}$ (5.0 g), NaH_2PO_2 (24.4 g) and NaAc (2.9 g) were dissolved in deionized water (100 mL) in a three-necked flask under a nitrogen atmosphere. The pH value was adjusted to 8 by the careful addition of potassium hydroxide (KOH) solution. The solution was heated to 90 °C under a nitrogen atmosphere, and the temperature was kept at 90 °C for 1 h. The temperature of the solution was then allowed to cool to room temperature. The precipitates were separated by centrifugation and washed with ammonia solution (25 – 28 wt%) and deionized water. Then it was dried in vacuum at 60 °C for 12 h and then annealed at 500 °C for 1 h under a nitrogen atmosphere in a tube furnace at a heating rate of 10 °C min^{-1} and a nitrogen flow rate of 100 sccm ($\text{cm}^3 \text{min}^{-1}$, 20 °C). Electrochemical measurements was performed using a three electrode configuration by PCI4/300™ potentiostat with PHE200™ software (Gamry Electronic Instruments, Inc.). Working electrode was prepared by dispersion of the catalyst (4 mg) and Nafion on solution (5 wt%, 80 mL) in 1 mL of water/ethanol ($4/1$, v/v) was ultrasonicated using an ultrasonic probe for 1 h to form a homogeneous ink, and then 5 mL of the ink was dropped onto the polished GCE. Pt mesh as the counter electrode and Ag/AgCl as the reference electrode.

Table S10 Optimized crystallographic parameters of Ni₃P compared with experimental data. The atomic fractional coordinates of all atoms and the bond lengths are also presented.

	Crystallographic parameters			Atomic fractional coordinates				Bond length
	a/ Å	b/ Å	c/ Å	Ni1	Ni2	Ni3	P	Ni-P/ Å
This work	8.954	8.954	4.386	(0.0775, 0.1117, 0.2609)	(0.1351, 0.4679, 0.0235)	(0.3311, 0.2800, 0.2476)	(0.2862, 0.0487, 0.0193)	2.277,2.277 2.323,2.323 2.281,2.222 2.313,2.323
Power neutron diffraction(Co K α) ^{S2}	8.950	8.950	4.385	(0.0783, 0.1132, 0.252)	(0.1349, 0.469,0. 028)	(0.2869, 0.0458, 0.02)	(0.3323, 0.2799, 0.25)	2.208,2.221 2.278,2.286 2.289,2.322 2.324,2.335
Powder X-ray diffraction (Cu K α) ^{S3}	8.954	8.954	4.386	(0.0775, 0.1117, 0.2609)	(0.1351, 0.4679, 0.0235)	(0.3311, 0.2800, 0.2476)	(0.2862, 0.0487, 0.0193)	2.208,2.221 2.279,2.287 2.291,2.322 2.326,2.335
Powder X-ray diffraction (Fe K) ^{S4}	8.916	8.916	4.389	(0.0775, 0.1117, 0.2609)	(0.1351, 0.4679, 0.0235)	(0.3311, 0.2800, 0.2476)	(0.2862, 0.0487, 0.0193)	2.202,2.214 2.271, 2.291 2.312, 2.326 2.327, 2.331

As shown in Table S10, the simulated crystallographic parameters of the optimized Ni₃P agree well with the experimental results from Powder X-ray diffraction. The slight difference is due to the error in experimental measurement and the approximations in theoretical calculation.

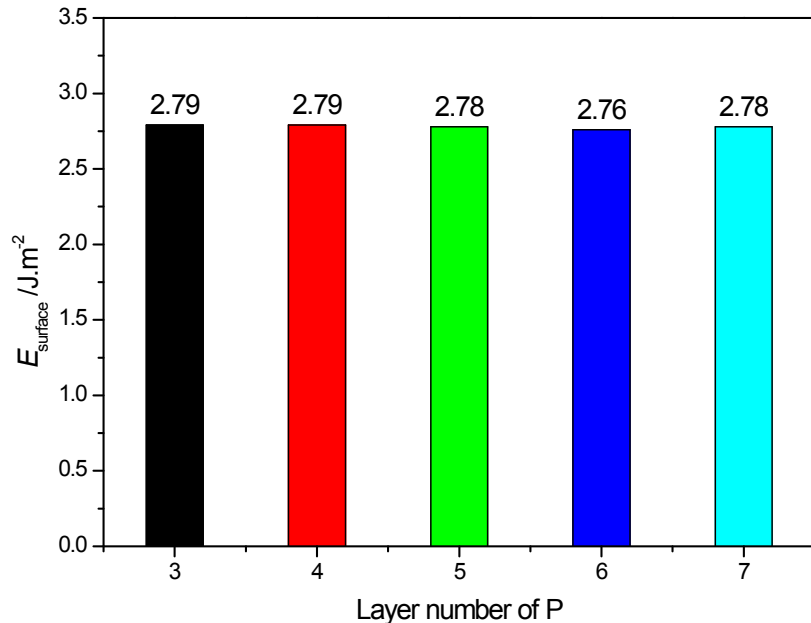


Figure S14. Surface energies of the (001)B facets with different supercell when the $\Delta\mu_P$ equals to -1.78 eV. The differences are quite small when the supercell contain more than five P layers (difference within the error bars of our slab model). Therefore, at least five P layers were selected during the simulation.

Table S11. The calculated energies of different species.

Species	Energy / eV.atom ⁻¹	Species	Formation Energy / eV.atom ⁻¹
Bulk Ni	-1355.276	Ni ₂ P	-0.478
Black P	-179.674	Ni ₅ P ₄	-0.481
Bulk Ni ₃ P	-1061.821	NiP	-0.436
H ₂	-31.867	NiP ₂	-0.376
Ni ₃ P	-0.445	NiP ₃	-0.304
Ni ₈ P ₃	-0.461	NiP ₄	-0.168
Ni ₁₂ P ₅	-0.481		

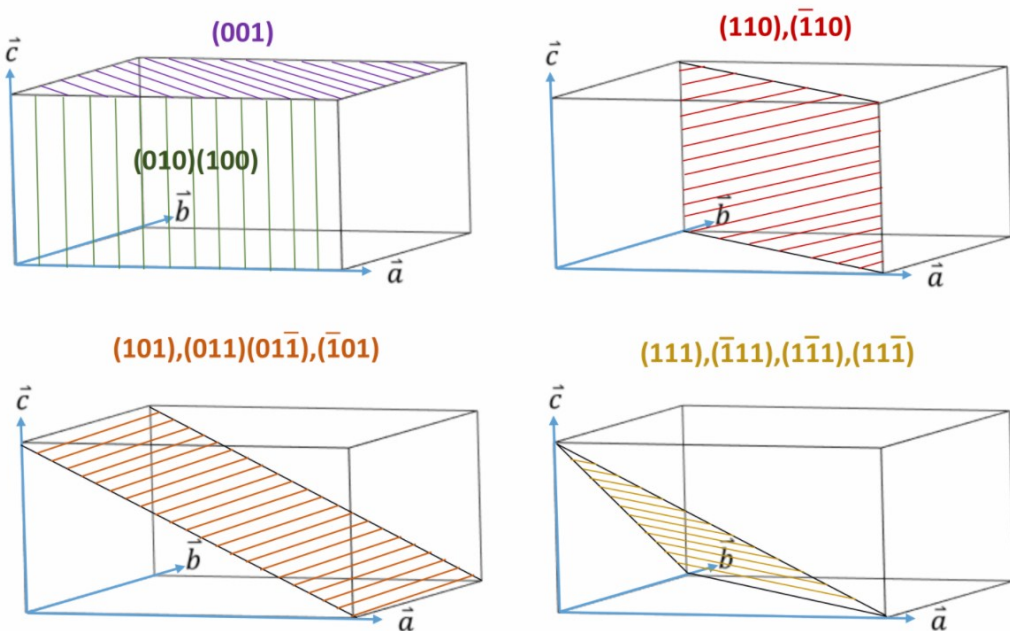


Figure S15. The overall surfaces considered in this paper, where equivalent surfaces (family of planes) are put together. Based on the symmetry of Ni₃P, the following planes are equivalent: the (010) and (100); the (110) and (bar{1}10); the (101), (011), (01bar{1}) and the (bar{1}01); (111), (bar{1}11), (1bar{1}1) and (bar{1}bar{1}1). Therefore, we only selected the (001), (010), (110), (101) and (111) surfaces during calculation.

References

- (S1) L. Jin, H. Xia, Z. Huang, Lv, C.; J. Wang, M. G.; Humphrey and C. Zhang, *J. Mater. Chem. A* 2016, 4, 10925–10932.
- (S2) R. Skala and M. Drabek, *Mineralogical Magazine* 2003, 67, 783–792.
- (S3) L. M. Yupko, A. A. Svirid and S.V. Muchnik, *Poroshkovaya Metallurgiya (Kiev)* 1968, 9, 78–83.
- (S4) H. Nowotny, E. Henglein. *Zeitschrift für Physikalische Chemie, Abteilung B* 1938, 40, 281–284 (in German).